J. Fluid Mech. (2004), *vol.* 498, *pp.* 1–21.
DOI: 10.1017/S0022112003007006 Printed in the United Kingdom

Vortex dynamos

By STEFAN G. LLEWELLYN SMITH[1] AND S. M. TOBIAS[2]

[1]Department of Mechanical and Aerospace Engineering, Jacobs School of Engineering, UCSD, 9500 Gilman Drive, La Jolla CA 92093-0411, USA

[2]Department of Applied Mathematics, University of Leeds, Woodhouse Lane, Leeds LS2 9JT, UK

(Received 14 August 2002 and in revised form 7 March 2003)

We investigate the kinematic dynamo properties of interacting vortex tubes. These flows are of great importance in geophysical and astrophysical fluid dynamics: for a large range of systems, turbulence is dominated by such coherent structures. We obtain a dynamically consistent $2\frac{1}{2}$-dimensional velocity field of the form $(u(x, y, t), v(x, y, t), w(x, y, t))$ by solving the z-independent Navier–Stokes equations in the presence of helical forcing. This system naturally forms vortex tubes via an inverse cascade. It has chaotic Lagrangian properties and is therefore a candidate for fast dynamo action. The kinematic dynamo properties of the flow are calculated by determining the growth rate of a small-scale seed field. The growth rate is found to have a complicated dependence on Reynolds number Re and magnetic Reynolds number Rm, but the flow continues to act as a dynamo for large Re and Rm. Moreover the dynamo is still efficient even in the limit $Re \gg Rm$, providing Rm is large enough, because of the formation of coherent structures.

1. Introduction

The origin of magnetic fields in astrophysical bodies is one of the fundamental problems of magnetohydrodynamics. It is widely believed that cosmical magnetic fields in objects as diverse as planets (including the Earth), stars, galaxies and accretion disks are sustained by dynamo action (see e.g. Roberts & Soward 1992; Weiss 2002). A dynamo is a system in which magnetic field is maintained within an electrically conducting fluid against the action of ohmic dissipation by the motions in the fluid (Moffatt 1978). Field-lines are stretched by straining motions within the fluid, leading to amplification of the magnetic field.

Dynamo theory has traditionally been divided into two regimes: kinematic and dynamic. The *kinematic* dynamo problem addresses whether a prescribed velocity field, $\boldsymbol{u}$, leads to amplification of a magnetic field, $\boldsymbol{B}$. This is an approximation because the back-reaction of the magnetic field on the flow is neglected. The induction equation then leads to exponentially growing or decaying magnetic fields. This simplified problem is nevertheless non-trivial, because the nature of dynamo action is subtle. For example many anti-dynamo theorems exist, of which the most famous is Cowling's Theorem of 1934. These preclude the magnetic field generated by dynamo action, or the velocity field that leads to dynamo action, from being too simple (see Roberts 1994, for a review of the subtleties of dynamo action). Once the magnetic field has grown to a sufficient level, it will act back on the fluid flow via the Lorentz force which is quadratic in the magnetic field. Determining the saturated magnetohydrodynamic

state of the coupled flow–magnetic field system requires a *dynamic* calculation (see e.g. Brummell, Cattaneo & Tobias 2001). With the advent of high performance computing, it is now possible to produce fully self-consistent dynamo solutions, albeit at relatively low Reynolds number and magnetic Reynolds number (*Re* and *Rm* respectively).

One problem that is better addressed within the confines of kinematic theory is the fast dynamo problem (see e.g. Childress & Gilbert 1995). In its simplest form, the fast dynamo problem determines whether a velocity field that is capable of dynamo action remains so in the limit of high, but not infinite, magnetic Reynolds number. Traditionally this problem has been attacked by considering the dynamo properties of prescribed velocities such as the ABC flow (Galloway & Frisch 1984) or time-dependent modifications thereof (Galloway & Proctor 1992). Such flows are carefully constructed to have properties conducive to dynamo action. The fast dynamo properties of geophysically and astrophysically realistic flows have not received nearly as much attention (although see Kim, Hughes & Soward 1999; Ponty, Gilbert & Soward 2001). In this paper we address the dynamo behaviour of one of the most common flows in geophysics and astrophysics: interacting vortex tubes.

Vorticity plays a key role in many geophysical and astrophysical flows. In three-dimensional turbulence, the dynamics is often dominated by the formation of coherent structures associated with vorticity (Vincent & Meneguzzi 1991; Frisch 1995). Understanding the interaction of these structures is then a central theme for turbulence theory. However in geophysical flows, which are dominated by strong stratification or by rotation, the flow is largely two-dimensional and vortex patches form in an inverse cascade from small scales (McWilliams 1984). The dynamics is again mediated by vortex interactions on the large scale. The presence of strong rotation and stratification can inhibit vertical velocities in stably stratified systems. In turn these small vertical velocities may reduce the efficiency of dynamo action for these flows. However in systems that are unstably stratified, vertical velocities are not necessarily small and efficient dynamo action is to be expected. An example of such a system where vortex tubes play an important role comes from astrophysical convection. Here the flow takes the form of strong vortical downflows dominating the dynamics and slower upflows that have a more passive role. The asymmetry between upflows and downflows is due to the compressible and stratified nature of the flow (Brummell, Cattaneo & Toomre 1995; Brummell, Clune & Toomre 2002). As a result, the downflows are much stronger than the upflows, and are associated with a large vorticity and hence helicity. These vortical downflows are apparent in observations of solar convection, appearing at the corners of the network of downflow lanes (Simon & Weiss 1997). In non-rotating convection, there is no overall handedness to the vorticity of the downflows, but the addition of rotation will yield a net helicity for the flow and lead to the possibility of large-scale dynamo action (Moffatt 1978). Even in the case of no overall net helicity it is to be expected that the strong vortices will be important for the generation of small-scale field, being the sites of strongest advection in the flow. On a larger scale still, vortices are expected to play a significant role in the magnetohydrodynamic turbulence responsible for accretion in accretion disks (see e.g. Bracco *et al.* 1999; Godon & Livio 2000; Balmforth & Korycansky 2001) and the formation of planets in protoplanetary disks (Li *et al.* 2001).

Because of their obvious importance, vortex dynamos have previously been studied in great detail. The archetypal model of a vortex dynamo was proposed by Ponomarenko (1973), who examined the kinematic dynamo properties of a rigid cylinder moving in a conducting medium. This model has been extended and refined in many subsequent papers (Ruzmaikin, Sokoloff & Shukurov 1988; Gilbert 1988) to

the more general case of kinematic dynamo action for a prescribed *steady* flow with helical streamlines. The velocity field is then given by

$$\boldsymbol{u} = (0, r\Omega(r), w(r)) \tag{1.1}$$

in cylindrical polar coordinates (r, ϕ, z), with $\Omega(r)$ the angular and w the axial (vertical) velocities respectively. This class of velocity is capable of supporting dynamo action. (Indeed the nonlinear properties of such a dynamo have recently been investigated by Bassom & Gilbert 1997; Dobler, Shukurov & Brandenburg 2002.) However the dynamo action for (1.1) relies on the presence of the diffusion term, and the growth rate for a mode with fixed wavenumber tends to zero as $Rm \to \infty$.

In this paper we investigate fast dynamo properties of a geophysically realistic flow field – interacting vortices – that is not prescribed, but arises as a natural solution to the Navier–Stokes equations at moderate to high Re. For a dynamo we require that the flow have all three components non-zero (Zel'dovich 1956), but, in order to reach the high values of Rm required to investigate fast dynamo action, we simplify the flow by considering a flow independent of depth (z). This leads naturally to what might be called $2\frac{1}{2}$-dimensional dynamics. It should be noted that this is significantly different to earlier studies (Kinney & McWilliams 1998) that investigated the effect of an *imposed* magnetic field on the dynamics of two-dimensional vortices – here the field is itself generated by the vortices themselves and all three components of the flow are non-zero.

In § 2 we set up the model, and derive the relevant hydromagnetic equations, as well as evolution equations for integral quantities. In § 3 we describe the purely hydrodynamic behaviour of these equations for a selection of different Re. We show that the solutions take the form of interacting vortices with complicated spatio-temporal dynamics. We then calculate the Lagrangian properties of the flow, which provide an important measure for the potential fast dynamo properties of the flow. In § 4 the kinematic dynamo properties of these flows are investigated, and we determine how the dynamo properties of the flow change as the magnetic Reynolds number and fluid Reynolds number are varied. We conclude in § 5 by examining the consequences of our results for astrophysical and geophysical dynamos and describing further calculations to be performed.

2. Set-up of the model: formulation, equations and numerical scheme

2.1. *Hydrodynamic equations*

We consider a $2\frac{1}{2}$-dimensional velocity field, by which we mean a field in which the velocity has three components,

$$\boldsymbol{u} \equiv (u(x, y, t), v(x, y, t), w(x, y, t)), \tag{2.1}$$

but does not depend on the z-coordinate. Note that this definition of $2\frac{1}{2}$-dimensional dynamics differs from that customarily used in the geodynamo literature, where $2\frac{1}{2}$-dimensional has come to mean that the flow and field are severely truncated in one direction.

The vorticity then takes the form

$$\boldsymbol{\omega} \equiv (w_y, -w_x, v_x - u_y). \tag{2.2}$$

The incompressible Navier–Stokes equations may be transformed into the vorticity equation and the incompressibility condition

$$\boldsymbol{\omega}_t + \boldsymbol{u}\cdot\nabla\boldsymbol{\omega} = \boldsymbol{\omega}\cdot\nabla\boldsymbol{u} + \nu\nabla^2\boldsymbol{\omega} + \nabla\times\boldsymbol{F}, \tag{2.3a}$$

$$\nabla\cdot\boldsymbol{u} = 0, \tag{2.3b}$$

where ν is the kinematic viscosity and $\nabla\times\boldsymbol{F}$ is the curl of any body forces present. In this paper we consider only the kinematic dynamo problem, so the back-reaction of the Lorentz force on the flow is ignored.

The set of equations (2.3) may be recast as evolution equations for the vertical component of the vorticity, $q \equiv v_x - u_y$, and the Laplacian of the vertical velocity, $\nabla^2 w$. The resulting equations are

$$q_t + \boldsymbol{u}\cdot\nabla q = \nu\nabla^2 q + (\nabla\times\boldsymbol{F})\cdot\hat{\boldsymbol{z}}, \tag{2.4a}$$

$$(\nabla^2 w)_t + \nabla^2(\boldsymbol{u}\cdot\nabla w) = \nu\nabla^4 w + \nabla^2 F_z, \tag{2.4b}$$

$$\nabla\cdot\boldsymbol{u} = 0. \tag{2.4c}$$

The vertical component of the curl of the forcing term $\boldsymbol{F}$ is $G_z \equiv (\nabla\times\boldsymbol{F})\cdot\hat{\boldsymbol{z}}$, while F_z is the z-component of $\boldsymbol{F}$.

We now assume that the vertical velocity contains no irrotational component, which is equivalent to the assumption that there is no pressure gradient in the z-direction. As a result, (2.4b) becomes the vertical velocity equation in the absence of a pressure gradient.

From the continuity equation, we write the horizontal velocity field in terms of a streamfunction, ψ, yielding

$$u = -\psi_y, \qquad v = \psi_x, \qquad q = \nabla^2\psi. \tag{2.5}$$

The governing equations may then be rewritten as

$$q_t + J(\psi, q) = \nu\nabla^2 q + G_z, \tag{2.6a}$$

$$w_t + J(\psi, w) = \nu\nabla^2 w + F_z, \tag{2.6b}$$

$$q = \nabla^2\psi. \tag{2.6c}$$

The Jacobian J is defined by $J(a,b) \equiv a_x b_y - a_y b_x$. The equation for q (equation (2.6a)) is the two-dimensional vorticity equation, while the equation for w (equation (2.6b)) is the advection equation for a passive scalar.

The $2\frac{1}{2}$-dimensional velocity field $\boldsymbol{u}$ is a candidate for dynamo action, since it has the three components necessary to be a dynamo (Zel'dovich 1956). Flows resulting from two-dimensional fluid motion are known to possess chaotic Lagrangian properties (Provenzale 1999), so the velocity field $\boldsymbol{u}$ is also a candidate for fast dynamo action for which the presence of chaotic trajectories is a necessary condition (Vishik 1989; Klapper & Young 1995). In § 3, we investigate the Lagrangian properties of the three-dimensional flow.

2.2. *Hydrodynamic integral quantities*

In the absence of dissipation, the set of equations (2.6) possesses several invariant quantities (Salmon 1998). We now examine the evolution equations for these quantities in the presence of dissipation. We call the area of the domain A and assume periodic boundary conditions.

We define the kinetic energy, $\mathscr{E}$, as the average over the domain of $\frac{1}{2}(u^2 + v^2 + w^2)$. The contribution to the kinetic energy due to the horizontal component of the flow

decays in the case of unforced flow, since

$$A\frac{\mathrm{d}\mathscr{E}_H}{\mathrm{d}t} = \frac{\mathrm{d}}{\mathrm{d}t}\int \tfrac{1}{2}|\nabla\psi|^2\,\mathrm{d}^2x = -\nu\int q^2\,\mathrm{d}^2x + \int (uF_x + vF_y)\,\mathrm{d}^2x. \tag{2.7}$$

The term due to viscous dissipation is negative definite. Similarly, the portion of the energy associated with the vertical component of the motion obeys the equation

$$A\frac{\mathrm{d}\mathscr{E}_V}{\mathrm{d}t} = \frac{\mathrm{d}}{\mathrm{d}t}\int \tfrac{1}{2}w^2\,\mathrm{d}^2x = -\nu\int |\nabla w|^2\,\mathrm{d}^2x + \int wF_z\,\mathrm{d}^2x \tag{2.8}$$

and must also decrease in time for unforced flow. This corresponds to the result that passive scalar variance must decrease in time in the absence of sources. To maintain statistically steady turbulence, we must apply a body force to the system that is parallel to the velocity field and hence injects energy into the flow.

Inviscid two-dimensional turbulence also conserves enstrophy, which is defined as the average of $\frac{1}{2}|\boldsymbol{\omega}|^2$ over the domain. The horizontal portion of the enstrophy satisfies

$$A\frac{\mathrm{d}\mathscr{Z}_H}{\mathrm{d}t} = \frac{\mathrm{d}}{\mathrm{d}t}\int \tfrac{1}{2}q^2\,\mathrm{d}^2x = -\nu\int |\nabla q|^2\,\mathrm{d}^2x + \int qG_z\,\mathrm{d}^2x. \tag{2.9}$$

However, the vertical portion of the enstrophy behaves rather differently. The advective term does not vanish and the resulting evolution equation is

$$A\frac{\mathrm{d}\mathscr{Z}_V}{\mathrm{d}t} = \frac{\mathrm{d}}{\mathrm{d}t}\int \tfrac{1}{2}|\nabla w|^2\,\mathrm{d}^2x = -\nu\int (\nabla^2 w)^2\,\mathrm{d}^2x - \int \frac{\partial w}{\partial x_j}e_{jk}\frac{\partial w}{\partial x_k}\,\mathrm{d}^2x + \int \nabla w\cdot\nabla F_z\,\mathrm{d}^2x, \tag{2.10}$$

where e_{ij} is the symmetric rate-of-strain tensor. The viscous term again decays, but the second integral on the right-hand side is not necessarily negative. Thus the total enstrophy of the unforced system can increase.

Finally the helicity is an inviscid invariant. The helicity integral is

$$A\mathscr{H} \equiv \int \tfrac{1}{2}\boldsymbol{u}\cdot\boldsymbol{\omega}\,\mathrm{d}^2x = \int wq\,\mathrm{d}^2x. \tag{2.11}$$

Unlike kinetic energy and enstrophy, helicity is not positive-definite. It evolves according to

$$A\frac{\mathrm{d}\mathscr{H}}{\mathrm{d}t} = -2\nu\int \nabla w\cdot\nabla q\,\mathrm{d}^2x + \int (wG_z + qF_z)\,\mathrm{d}^2x. \tag{2.12}$$

The terms on the right-hand side of (2.12) are not sign-definite, and helicity can increase or decrease for freely decaying as well as forced flows. Taking vertical velocity as a passive scalar, helicity conservation in the unforced inviscid case corresponds to the conservation of correlation between vorticity and passive scalar.

2.3. *Magnetic equations*

The governing equation for the solenoidal magnetic field is the induction equation, and hence, as the flow is incompressible,

$$\boldsymbol{B}_t + \boldsymbol{u}\cdot\nabla\boldsymbol{B} = \boldsymbol{B}\cdot\nabla\boldsymbol{u} + \eta\nabla^2\boldsymbol{B}, \tag{2.13a}$$

$$\nabla\cdot\boldsymbol{B} = 0, \tag{2.13b}$$

where η is the magnetic diffusivity. As the flow is two-dimensional, we may decompose the magnetic field into Cartesian coordinates with imposed vertical wavenumber k according to

$$\boldsymbol{B} = (b_1, b_2, b_3)\mathrm{e}^{\mathrm{i}kz} + \text{c.c.}, \tag{2.14}$$

where c.c. stands for complex conjugate. The components b_1, b_2 and b_3 are functions only of x and y.

The equations (2.13) reduce to two coupled equations and the solenoidal condition,

$$b_{1t} + J(\psi, b_1) + \mathrm{i}kwb_1 = -\psi_{xy}b_1 - \psi_{yy}b_2 + \eta(\nabla^2 - k^2)b_1, \tag{2.15a}$$

$$b_{2t} + J(\psi, b_2) + \mathrm{i}kwb_2 = \psi_{xx}b_1 + \psi_{xy}b_2 + \eta(\nabla^2 - k^2)b_2, \tag{2.15b}$$

$$b_3 = \frac{\mathrm{i}}{k}(b_{1x} + b_{2y}), \tag{2.15c}$$

where ∇^2 is the horizontal part of the Laplacian operator as before. The action of the vertical part of the Laplacian operator gives the $-k^2$ terms in (2.15).

2.4. *Magnetic integral quantities*

The magnetic energy, $\mathscr{E}_M$, is defined to be the average of $\frac{1}{2}\boldsymbol{B}\cdot\boldsymbol{B}$ over the domain. The magnetic field depends on z, so we also include an average in the vertical over an extent $2\pi/k$. Consequently

$$A\mathscr{E}_M \equiv \frac{k}{2\pi}\int_0^{2\pi/k}\int \tfrac{1}{2}|\boldsymbol{B}|^2\,\mathrm{d}^2x\,\mathrm{d}z = \int (|b_1|^2 + |b_2|^2 + |b_3|^2)\,\mathrm{d}^2x. \tag{2.16}$$

A vector potential $\boldsymbol{A} \equiv (a_1, a_2, 0)\mathrm{e}^{\mathrm{i}kz} + \text{c.c.}$ may be defined by choosing a convenient gauge, giving

$$b_1 = -\mathrm{i}ka_2, \qquad b_2 = \mathrm{i}ka_1. \tag{2.17}$$

The magnetic helicity is then

$$A\mathscr{H}_M \equiv \frac{k}{2\pi}\int_0^{2\pi/k}\int \boldsymbol{A}\cdot\boldsymbol{B}\,\mathrm{d}^2x\,\mathrm{d}z = \frac{4}{k}\int \mathrm{Im}(b_1^* b_2)\,\mathrm{d}^2x. \tag{2.18}$$

We shall not force the induction equations in (2.15), and the growth of the magnetic field is due entirely to its straining by the velocity field. The growth in the magnetic energy will be our indicator for the dynamo properties of the system.

2.5. *Numerical scheme*

We solve the system of equations (2.6) and (2.15) in a periodic domain with side 2π, using an extension of the scheme of Hua & Haidvogel (1986). This is a spectral method, with the dynamic variables q, w, b_1 and b_2 represented as sums of Fourier modes. The governing equations are solved using a leapfrog step for the advective terms and a trapezoidal step for the dissipative terms. The nonlinear terms are computed in physical space (i.e. pseudospectrally). A leapfrog trapezoidal step is applied periodically to diminish the computational mode. The evolution of the real and imaginary parts of b_1 and b_2 are computed separately. The passive tracer equation for w and induction equations for b_1 and b_2 are linear equations, but the advective terms still require pseudospectral treatment since the different modes couple in Fourier space, and are treated in physical space as in the vorticity equation.

The flow is not prescribed and it arises naturally as a result of the forcing. We therefore have no prior knowledge of the amplitude of the solution. The Reynolds number and magnetic Reynolds number of the flow can therefore not be prescribed, but must be calculated *a posteriori*, in much the same way as in Rayleigh–Bénard convection where the diffusivities and thermal driving are prescribed and the Reynolds numbers can only be calculated after the fact. Here the Reynolds and magnetic

Reynolds numbers are defined by

$$Re = \frac{\langle \boldsymbol{u}^2 \rangle^{1/2} L}{\nu}, \quad Rm = \frac{\langle \boldsymbol{u}^2 \rangle^{1/2} L}{\eta}, \tag{2.19}$$

where $\langle \boldsymbol{u}^2 \rangle$ denotes a temporal as well as spatial average. The lengthscale for the vortices in the velocity field will turn out to be slightly less than the lengthscale of the domain and so Reynolds numbers quoted will be slightly larger than a Reynolds number defined on the length scale of the flow. To avoid confusion, both the prescribed diffusivities and the resulting Reynolds numbers will be quoted for each calculation (see table 1 below).

Calculations for the evolution of the velocity and magnetic field are typically started from random initial conditions. Here the initial conditions for the horizontal velocity have random phase and amplitudes drawn from the isotropic kinetic energy spectrum of McWilliams (1990). The vertical velocity is taken from the same distribution, as are the real parts of b_1 and b_2. To a certain extent, the exact form of the initial conditions is not crucial, since vortices will condense out of most initial conditions (Arroyo *et al.* 1995).

Many previous simulations of two-dimensional turbulence have used hyperviscosity, i.e. dissipative terms of the form ∇^{2n} with $n > 1$, to increase the Reynolds number (McWilliams 1984). There are possible pitfalls in this approach, since such operators do not preserve the monotonic decay of free turbulence. Since our aim here is to investigate the dependence of the dynamo properties of the flow on the hydrodynamic and magnetic Reynolds numbers, we use only diffusion in the simulations.

3. Hydrodynamics of forced vortex flows

3.1. *Eulerian properties of the flow: alignment of w with vortices*

In this section we describe the hydrodynamic evolution of the velocity field that will be used in the kinematic dynamo simulations. In the absence of forcing, the presence of viscosity leads to decaying turbulence and the kinetic energy of the fluid decreases according to (2.7)–(2.8). To sustain dynamo action, we require non-decaying turbulence, so we impose a forcing on the horizontal and vertical velocities. For simplicity we choose to force the horizontal flow at wavenumber 4, as in Ohkitani (1991). Hence we set $G_z = G_0(\cos(4x) + \cos(4y))$, with the amplitude G_0 a free parameter. We select a similar forcing for the vertical velocity equation, $F_z = F_0(\cos(4x) + \cos(4y))$, and so the forcing is maximally helical (i.e. $G_z \propto F_z$). We expect the net helicity in the flow to evolve according to equation (2.12), and to be non-zero in the saturated state. For this choice of maximally helical forcing it is possible to remove some of the parameters by rescaling the equations. However, we prefer to retain all the parameters for future studies. Properties of flows where G_z is not proportional to F_z may be quite different and are currently being investigated, and will be reported in a future paper.

The evolution equations (2.6) for q and w are then integrated from random initial conditions. These initial conditions for q and w are different, and so the fields are initially uncorrelated. An example of the evolution of q and w is shown in figure 1 for the parameters $F_z = 0.25$, $G_z = 0.05$, $\nu = 0.004$. We shall hold the value of the forcing fixed for the rest of the paper. This is different in spirit to dynamo calculations where the forcing is altered in order to drive the same flow whatever the imposed viscosity (e.g. Brummell *et al.* 1998; Cattaneo, Hughes & Thelen 2002).

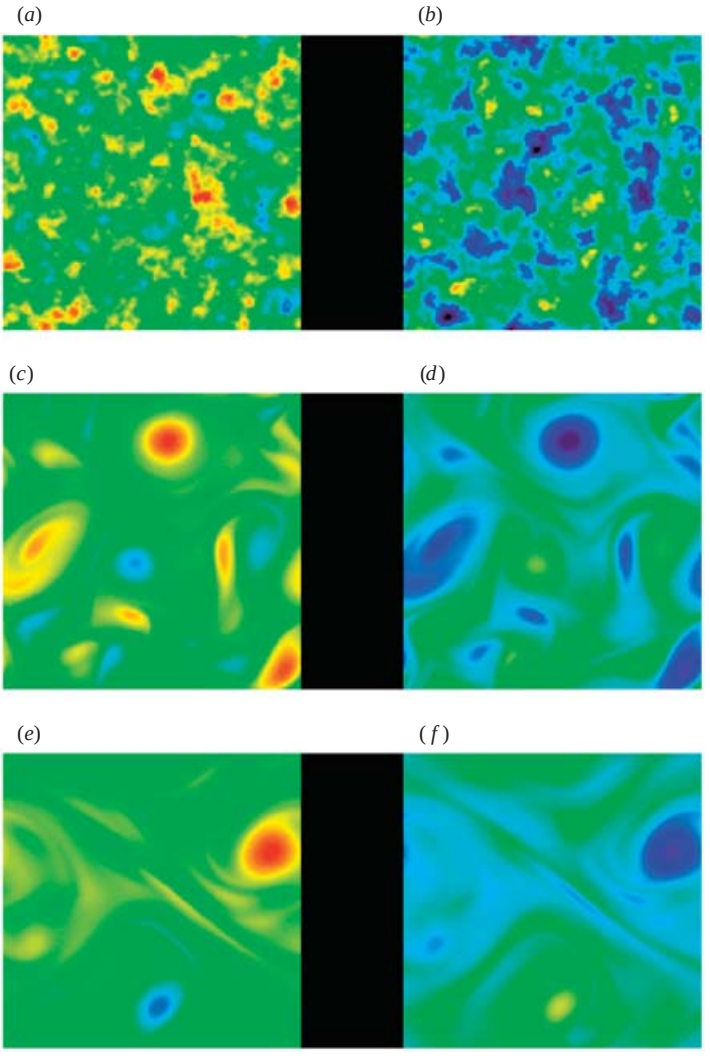

FIGURE 1. Evolution of the vertical vorticity and vertical velocity. The colour plots show the evolution of q (a, c, e) and w (b, d, f) from random initial conditions. The figures are snapshots taken at times $t = 0$ (a, b), $t = 10$ (c, d) and $t = 450$ (e, f). The inverse cascade mediated via vortex merging leads to the formation of two oppositely-signed interacting vortices. The vertical velocity becomes aligned (anti-correlated) with the vertical vorticity leading to a flow with a negative net helicity.

The vertical vorticity, q, which is initially small scale and random, evolves via an inverse cascade. A number of small vortices begin to condense out of the initial conditions as shown in figure 1(c). As the evolution continues, these vortices begin to interact and merge until only two oppositely signed vortices remain (figure 1e). These two vortices continue to interact with each other as a statistically steady state is reached. This inverse cascade and subsequent interaction for two-dimensional flows is well documented (McWilliams 1984; Babiano *et al.* 1987; McWilliams 1990; Ohkitani 1991; Arroyo *et al.* 1995; Provenzale 1999).

The evolution for the vertical velocity, w, is interesting however. As noted earlier, the evolution equation for w is mathematically similar to that for a passive scalar, and

we might expect similar behaviour. The vertical velocity is advected and stretched by the horizontal flow and is dissipated by viscosity. However the vertical velocity may take both signs of course (whereas passive scalars are usually of one sign), and w may also be expected to respond to the small-scale forcing, F_z. Figure 1(b, d, f) shows that the vertical velocity rapidly evolves from its random initial condition. The length scale of the vertical velocity increases and w begins to become anti-correlated with the vertical vorticity. As the vorticity inverse cascades to form two interacting vortex patches, so does the vertical velocity and by the time the statistically steady state is reached the vertical velocity is very well, though not perfectly, correlated with the vertical vorticity. The flow field therefore takes the form of interacting vortex tubes with throughflow.

The alignment of the vertical velocity with the vorticity is intriguing. The degree of correlation in two-dimensional turbulence between passive scalars and vorticity does not appear to be the subject of consensus. Babiano *et al.* (1987) claim there is no correlation. However the simulations of Holloway & Kristmannsson (1984) and Holloway, Riser & Ramsden (1986) suggest that tracer is being concentrated in vortex cores and strained between the cores. For unforced, inviscid flow, the integral of cq, where c is the concentration of passive scalar, does not change. The actual degree of correlation between vorticity and passive scalar probably depends on the initial conditions, the Péclet number (which is 1 here), the forcing, and the form of diffusion chosen. In this case of forced *maximally helical* turbulence with Péclet number unity it is simple to show that if $F_z = \lambda G_z$ then

$$\frac{\mathrm{d}}{\mathrm{d}t} \int \tfrac{1}{2}(w - \lambda q)^2 \, \mathrm{d}^2x = -\nu \int |\nabla(w - \lambda q)|^2 \, \mathrm{d}^2x, \tag{3.1}$$

and so rapid alignment takes place. Note that if the forcing is not maximally helical then no such manipulation is possible and the degree of alignment needs to be calculated by timestepping the equations. Physically, passive scalars become trapped in vortex cores, while any scalar trapped between the vortices is advected by stagnation-point flows back towards a vortex. For the vertical velocity, which is of both signs, the alignment is even more clear cut. The vertical velocity is advected as a passive scalar, but is also subject to cancellation. Within the vortex cores where the vertical velocity is largely of one sign there is little cancellation and the velocity can remain there. In the stagnation-point flows between the vortices, vertical velocities with opposite signs are often brought together and cancel, and so the vertical velocity is significantly reduced between the vortex cores. Hence the vertical velocity becomes strongly correlated with the vertical vorticity.

The evolution of the system to a statistically steady state was analysed for two further values of the viscosity: $\nu = 0.002$ and $\nu = 0.001$ (with F_z and G_z held constant). For these values the evolution follows a similar course to the first case, with an inverse cascade leading to the formation of a pair of interacting vortices. The kinetic energy of the system saturates when there is a balance between inertia, diffusion and forcing. This saturation is visible in figure 2, which shows the horizontal, vertical and total kinetic energies for the three values of viscosity. As expected from equations (2.7) and (2.8), decreasing the viscous dissipation leads to an increase in the kinetic energy of the vortices, and hence to a corresponding increase in the Reynolds number. For $\nu = 0.004$, 0.002 and 0.001, the calculated Reynolds numbers are $Re = 505$, 1280 and 2640, so it is clear that the Reynolds number is not simply inversely proportional to the viscosity. For this particular choice of forcing parameters the energy in the horizontal flow is larger than that in the vertical flow.

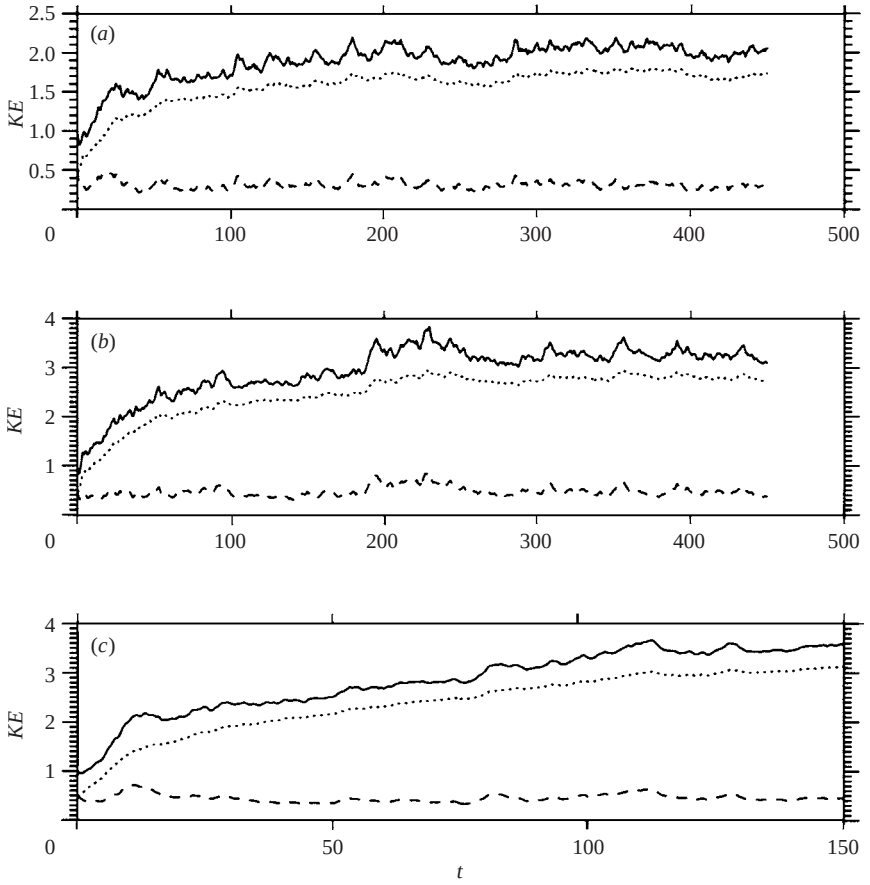

FIGURE 2. Kinetic energy of the flow. Time series of the evolution of the total kinetic energy (solid line), horizontal kinetic energy (dotted line) and vertical kinetic energy (dashed line) for (*a*) $\nu = 0.004$ ($Re = 505$), (*b*) $\nu = 0.002$ ($Re = 1280$) and (*c*) $\nu = 0.001$ ($Re = 2640$). In each case the energy settles down to a constant value as the velocity reaches a statistically steady state.

The steady helical forcing leads to an injection of helicity density at $k = 4$. The total kinetic helicity is shown in figure 3 for the three values of viscosity. For all these cases the basic evolution of the helicity is similar. The helicity is always negative because of the imposed forcing. During the inverse cascade the magnitude of the kinetic helicity increases for two reasons. The first is simply the increase in the amplitude of the horizontal and vertical flows. The second, more important, effect is the alignment of the vertical velocity with the vertical vorticity. This anti-correlation leads to the negative net helicity. While helicity is known to be an important factor in the generation of large-scale magnetic fields by promoting an inverse cascade in the magnetic field (see e.g. Moffatt 1978), it has been shown not to be critical to the generation of small-scale magnetic field (Hughes, Cattaneo & Kim 1996). However the presence of vorticity in coherent structures may aid dynamo action even on small scales, as we shall see in § 4.

The Eulerian properties of the flow field to be used in the kinematic dynamo studies are interesting, since the flow field is made up of interacting vortices that are reminiscent of many turbulent flows in geophysics and astrophysics. The spectra of

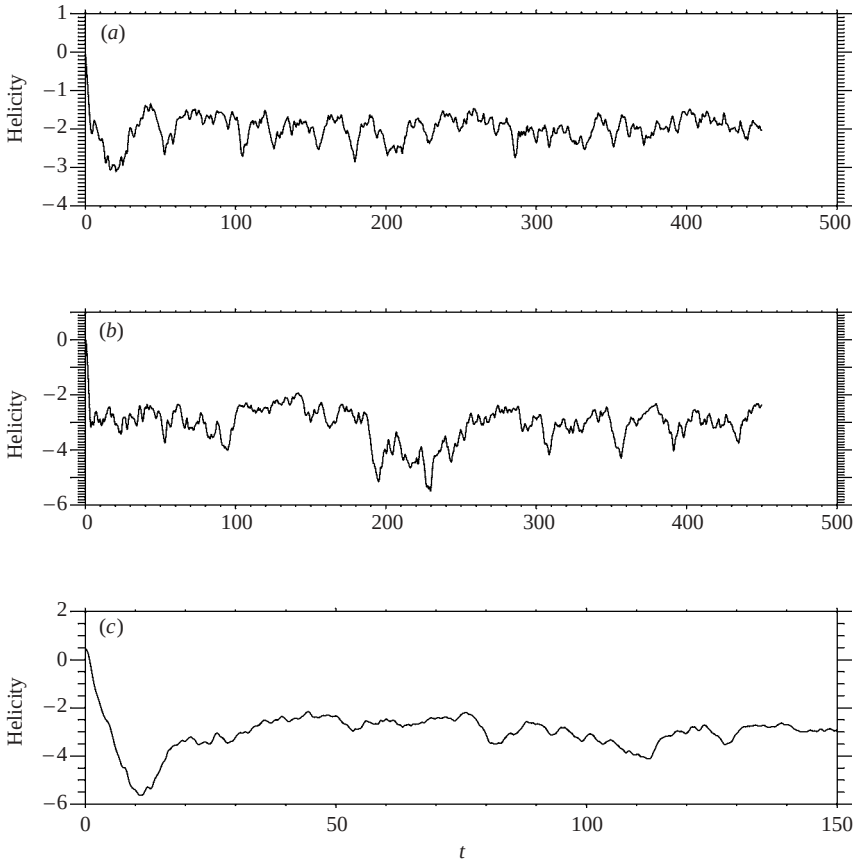

FIGURE 3. Overall helicity of the flow. Time series of the evolution of the total helicity for (*a*) $\nu = 0.004$ ($Re = 505$), (*b*) $\nu = 0.002$ ($Re = 1280$) and (*c*) $\nu = 0.001$ ($Re = 2640$). In each case there is a net (negative) helicity driven by the helical forcing.

dynamical variables such as vorticity and velocity have been extensively studied for two-dimensional turbulence. However, the spectra do not give the full picture, since they neglect the phase information required for a complete description of the coherent structures of turbulence. As a result, we have not computed spectra. In addition, for fast dynamo calculations, it is the Lagrangian properties of the flow that are most important. We analyse these in the next section.

3.2. *Lagrangian properties of the flow*

It is now well understood that for a flow to be a potential fast dynamo, it must possess regions of exponential stretching (Vishik 1989; Klapper & Young 1995). These regions are characterized by chaotic advection within the flow. To understand the stretching properties of the flow, we therefore calculate the finite-time Lyapunov exponents. This is achieved following the procedure outlined in Soward (1994; see also Brummell *et al.* 2001). We take a particle of fluid at an initial position $\boldsymbol{a}$ and calculate its trajectory. We then consider the evolution of the three-by-three Jacobian matrix $\boldsymbol{J}$, where $J_{ij}(\boldsymbol{a}, t) = \partial x_i / \partial a_j$, given by the equation

$$\frac{\mathrm{d}J_{ij}}{\mathrm{d}t} = \frac{\partial u_i}{\partial x_k} J_{kj} \tag{3.2}$$

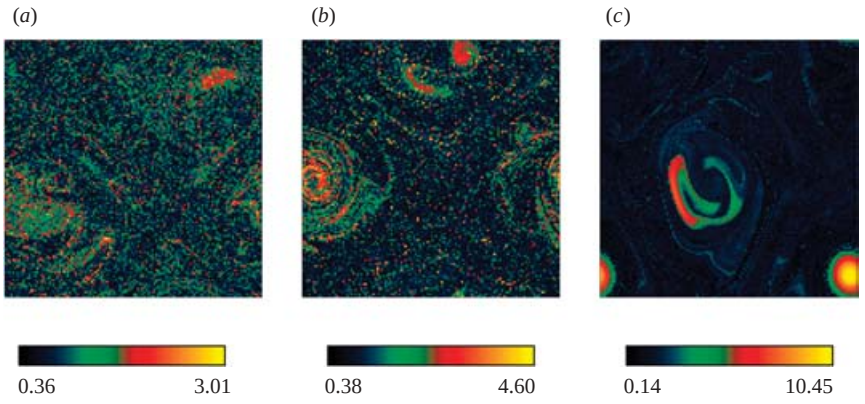

FIGURE 4. Lagrangian properties of the flow. Finite-time Lyapunov exponents as a function of initial position for a grid of 128^2 equally spaced particles with (*a*) $\nu = 0.004$ ($Re = 505$) with $t_0 = 50$, (*b*) $\nu = 0.002$ ($Re = 1280$) with $t_0 = 50$, and (*c*) $\nu = 0.001$ ($Re = 2640$) with $t_0 = 30$. In each case there are no integrable regions in the flow and chaotic trajectories are observed.

as the fluid moves along the particle paths. We define $\boldsymbol{\Lambda} \equiv \boldsymbol{J}^T \boldsymbol{J}$. Then the Lyapunov exponent is

$$\lambda(\boldsymbol{a}, \boldsymbol{e}) = \lim_{t\to\infty} \left(\frac{1}{2t} \ln(\boldsymbol{e} \cdot \boldsymbol{\Lambda} \cdot \boldsymbol{e}) \right), \tag{3.3}$$

where $\boldsymbol{e}$ is a suitably defined initial vector. The finite-time Lyapunov exponent is then defined in a similar manner, taking the final value of the time to be a fixed value t_0.

We repeat this calculation for an array of initial conditions once the flow has reached a statistically steady state. We *do* allow the flow to evolve in time as equation (3.2) is integrated, so u_i is a function of time. The results are shown in figure 4 for the three values of the viscosity. The first and most important result is that for all three flows there are significant regions of stretching as demonstrated by positive finite-time Lyapunov exponents. Indeed for all three flows the minimum value of the finite-time Lyapunov exponent is greater than zero. This implies that there are no integrable regions in the flow. The maximum values of the finite-time Lyapunov exponents are fairly large compared to the corresponding values for prescribed ABC flows (as are the average values, which are all $O(1)$). This is due to the large values of the strain that are achieved near the dynamic stagnation points between the interacting vortices. Some structure is also visible in the map of the finite-time Lyapunov exponents, especially for the $\nu = 0.001$ case in figure 4(*c*). Here the largest finite-time Lyapunov exponents appear to correlate with the initial position of the vortex patches. This is a slightly surprising result as most of the stretching occurs between the vortex patches and particles tend to remain trapped within vortex patches. However the dynamic and intermittent nature of the vortices means that particles can easily escape the vortices into the stretching regions between. It is clear, however, that these flows have exceedingly good stretching properties with large regions of Lagrangian chaos. One therefore expects them to make excellent small-scale dynamos.

4. Dynamo properties of the flow

In this section we examine the kinematic dynamo properties of the interacting vortex flow. We begin by describing in detail the dynamics for a particular choice

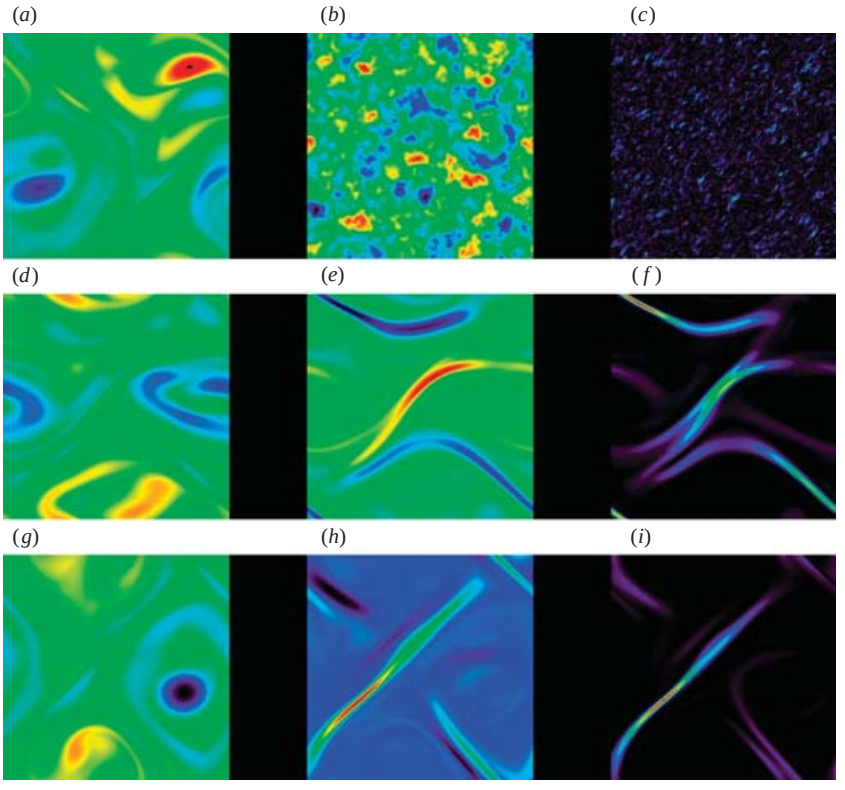

FIGURE 5. Evolution of the magnetic field. The figure shows the spatiotemporal evolution of the vertical vorticity q (a,d,g), Re(b_1) (b,e,h) and $\boldsymbol{B}\cdot\boldsymbol{B}$ (c,f,i) for $\nu = 0.004$, $\eta = 0.01$ and $k = 0.7$. The figures are snapshots taken at times $t = 450$ – the start of the dynamo calculation $(a–c)$ $t = 460$ $(d–f)$ and $t = 470$ $(g–i)$. The magnetic field is stretched and amplified by the interacting vortices. The exponential increase in the magnetic field and magnetic energy has been subtracted from these figures (i.e. these figures are scaled separately) so that the structure of the generated field can be seen.

of parameters ($\nu = 0.004$, $\eta = 0.01$, $k = 0.7$) before examining how the dynamo properties vary with changing parameters.

4.1. *The evolution and structure of a dynamo-generated magnetic field*

4.1.1. *Dependence of growth rate on Rm*

We start the hydromagnetic calculation from a mature solution to the hydrodynamic problem, such as the one shown in figure 1(e), where the energy and enstrophy of the flow have settled down to a statistically steady level. To this velocity field $\boldsymbol{u}(x, y, t)$ we add an initial seed magnetic field $\boldsymbol{B}_0(x, y)$ which is random, small scale and has zero horizontal mean (as shown in figure 5b,c). The seed field is drawn from the same distribution as the initial vertical vorticity. This magnetic field is immediately advected and stretched by the velocity field and begins to grow. After an initial transient, the field takes the form of thin strips of strong magnetic field found at the edges of the vortex tubes (see figure 5h,i). As the vortices interact and move, the magnetic field is advected with the vortices, continuing to be stretched and amplified near the stagnation points that are found in between the vortices. Both the velocity and magnetic field are highly time-dependent.

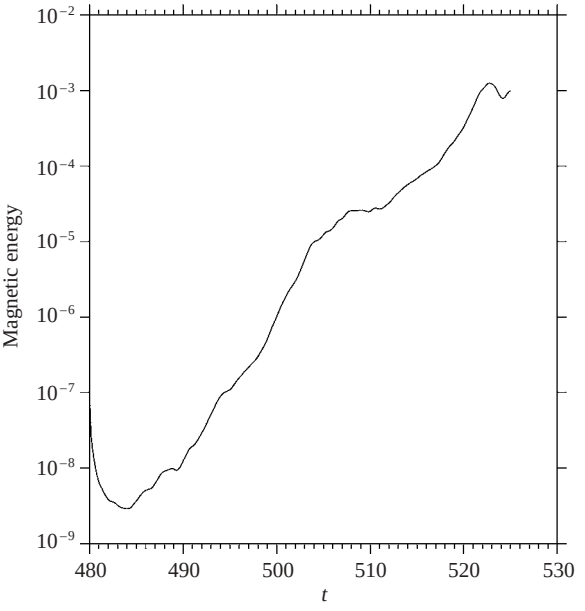

FIGURE 6. Evolution of the magnetic energy. Time series of the magnetic energy for the parameters given in figure 5.

For this choice of parameters the stretching by advection is sufficient to overcome the ohmic dissipation and the magnetic field begins to grow. As the effects of the Lorentz force have been neglected and the induction equation is linear, this growth is on average exponential. If the flow were steady, the growth would be exponential with a well-defined growth rate σ (see e.g. Galloway & Frisch 1984, who consider the dynamo properties of a steady ABC flow). If the flow were periodic (see e.g. Galloway & Proctor 1992), the growth rate σ would be the solution to a Floquet problem, and the evolution of the energy would take the form of exponential growth superimposed on an oscillation with the period of the underlying flow. Here the flow is unsteady and has no simple time-dependence, so the growth rate of the field can only be determined in an average sense. Figure 6 shows the evolution of the magnetic energy on a logarithmic scale over a long timescale for this choice of parameters. The average growth rate of the field σ is then obtained by fitting a straight line to this graph (having allowed the initial transients to die away), calculating the slope and dividing by 2. Error bars for the growth rate can be calculated by fitting straight lines to a number of sub-intervals of the time series and determining the maximum and minimum growth rate.

To determine how the dynamo properties of the flow depend on the parameters of the problem, we repeat the calculation described above for a variety of parameter choices. In particular we are interested in how the growth rate σ changes as a function of vertical wavenumber k, magnetic Reynolds number Rm and Reynolds number Re.

Figure 7 shows the growth rate σ as a function of k for fixed $\nu = 0.004$ (corresponding to $Re = 505$) and $\eta = 0.01$ (corresponding to $Rm = 202$). This figure shows that $\sigma \to 0$ as $k \to 0$, a result for $2\frac{1}{2}$-dimensional flows that was first established by Roberts (1972) who demonstrated that $\sigma = O(k)$ as $k \to 0$. As k increases, the growth rate increases to a maximum at $k = 0.9$ before decreasing again for larger k

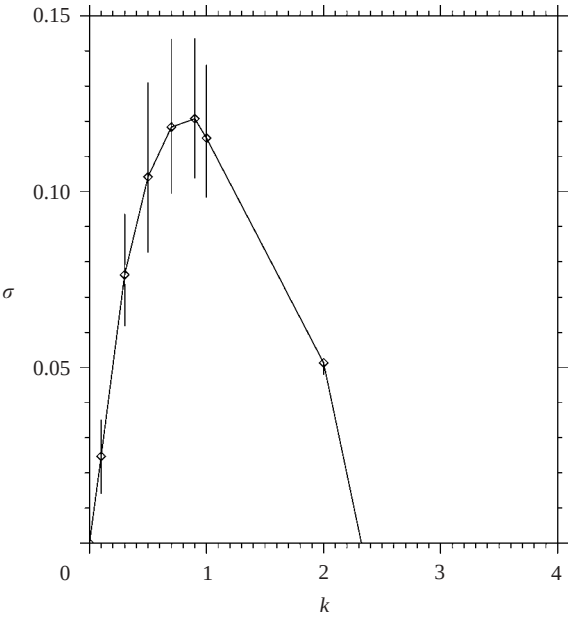

FIGURE 7. Growth rate versus k for $\nu = 0.004$, $\eta = 0.01$. The error bars are shown by vertical lines.

and eventually becoming negative for $k > 2$. For large k advection is not sufficient to overcome dissipation. This behaviour is typical of dynamos with velocity fields that vary on $O(1)$ horizontal lengthscales (e.g. Galloway & Proctor 1992; Hughes *et al.* 1996). Figure 8 shows that as Rm is increased, the growth rate grows for each k, and a second maximum in the growth rate can be found at $k = 3$. for $\eta = 0.001$ ($Rm = 2020$). The increase in magnetic Reynolds number leads to growing solutions at higher k, but it is noticeable that, for the primary maximum at $k = 0.9$, σ rapidly becomes independent of Rm. As Rm is increased further, the mode of overall highest growth rate switches between the two maxima and is now found for the higher k. For both of these wavenumbers the growth rate is still an increasing function of Rm, indicating the potential for fast dynamo action, but the growth rate at $k = 0.9$ appears to begin to saturate first, allowing the optimal mode to move to higher k. For sufficiently high Rm, the mode of maximum growth rate appears to become independent of Rm. This behaviour is more reminiscent of that of the Galloway–Proctor flows (where the growth rates stay largely independent of k for sufficiently high Rm) than the Ponomarenko dynamo. In the latter, the mode of maximum growth rate moves to higher and higher k as Rm is increased, and scales as $Rm^{1/3}$ for the continuous Ponomarenko dynamo (Gilbert 1988). In any case it seems that the growth rate for fixed wavenumber k stays bounded away from zero and that the flow is a good candidate for fast dynamo action. The spatial dependence of the magnetic field is also a function of η (and hence Rm) as shown in figure 9. As η is decreased, the lengthscale of the magnetic field decreases, scaling as $Rm^{-1/2}$ as it must in a kinematic calculation.

Although the flow is a reasonable dynamo, it is not as efficient as flows that are designed for dynamo action such as the Galloway–Proctor flow. For those flows, the growth rate has saturated by $Rm = O(10^2)$, while our freely evolving dynamic flows require $Rm = O(10^3)$ before the growth rate begins to saturate. It is possible that the

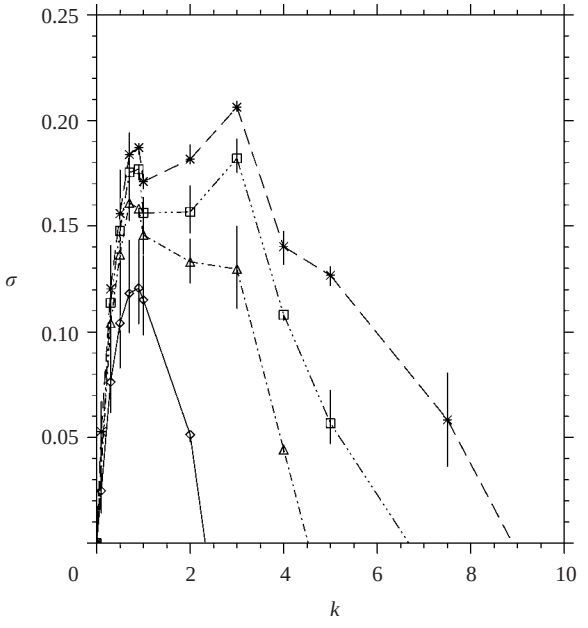

FIGURE 8. Growth rate versus k for $\nu = 0.004$, and $\eta = 0.01$ (solid line), $\eta = 0.002$ (dot-dashed line), $\eta = 0.001$ (dot-dot-dot-dashed line) and $\eta = 0.0005$ (dashed line). The error bars are shown by vertical lines.

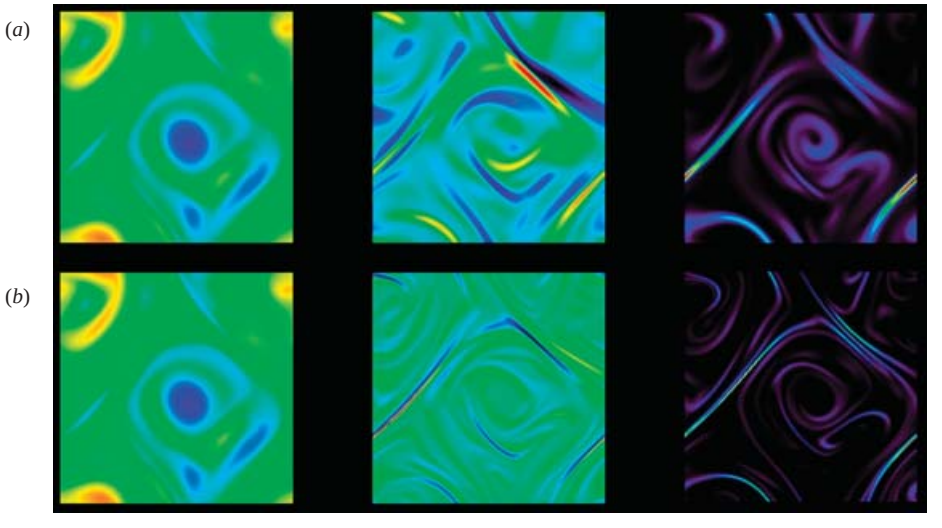

FIGURE 9. Structure of the magnetic field as a function of Rm. The colour snapshots show the evolution of the magnetic field for $\nu = 0.004$ for (a) $\eta = 0.01$ ($Rm = 202$), (b) $\eta = 0.001$ ($Rm = 2020$). The lengthscale of the field scales as $Rm^{-1/2}$.

growth rate σ would continue to increase as Rm is increased further. The growth rate for $Rm = 4040$ is, however, typical of the values achieved for kinematic fast dynamos with two-dimensional flows.

ν	η	Re	Rm	σ_c	k_c
0.004	0.01	505	202	0.241	0.9
0.004	0.002	505	1010	0.322	0.7
0.004	0.001	505	2020	0.364	3.0
0.004	0.0005	505	4040	0.412	3.0
0.002	0.01	1280	256	0.287	0.9
0.002	0.002	1280	1280	0.398	1.0
0.002	0.001	1280	2560	0.424	1.0
0.002	0.0005	1280	5120	0.442	3.0
0.001	0.01	2640	264	0.543	1.0
0.001	0.002	2640	1320	0.380	0.9
0.001	0.001	2640	2640	0.437	1.0
0.001	0.0005	2640	5280	0.478	1.0

TABLE 1. Imposed diffusivities and calculated Reynolds numbers (Re, Rm) with the maximum growth rate σ_c and the corresponding wavenumber k_c.

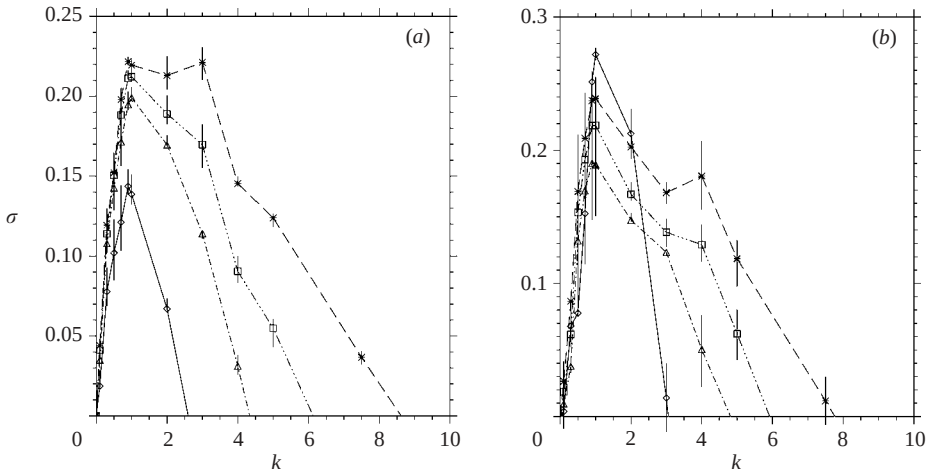

FIGURE 10. Growth rates as a function of k. As for figure 8 but here (a) $\nu = 0.002$ ($Re = 1280$), (b) $\nu = 0.001$ ($Re = 2640$).

4.1.2. *Dependence of growth rate on Re*

In this subsection we investigate how the dynamo properties change as the fluid Reynolds number Re is increased. In § 3 we examined the formation of vortices via an inverse cascade for three values of the viscosity $\nu = 0.004, 0.002, 0.001$ with the forcing held constant, which correspond to $Re = 505, 1280, 2640$. In each case coherent structures formed with an energy and helicity that were sensitive to the value of the viscosity.

We now repeat the calculations of § 4.1.1 for the parameter values $\nu = 0.002$ and 0.001. The results are summarized in table 1 and in figure 10, which shows growth rate against wavenumber k for various values of the magnetic diffusivity η (and hence Rm). Figure 10(a) shows the curves for $\nu = 0.002$, whilst figure 10(b) is for $\nu = 0.001$. Both figures have similar overall features to the $\nu = 0.004$ case shown in figure 8. The growth rate of the field is again a function of vertical wavenumber (for all values of

Re, Rm) with $\sigma \to 0$ as $k \to 0$ and $\sigma < 0$ as $k \to \infty$. For each value of η and ν, there is a mode, given by $k = k_c$ say, for which the growth rate is maximum ($\sigma = \sigma_c$). Again, for both new sets of parameter values, dynamo action occurs for a larger range of k as Rm is increased. Moreover, for $\nu = 0.002$ the mode of maximum growth rate switches between $k = 1.0$ and $k = 3.0$. For $\nu = 0.001$, however, $k = 1.0$ remains the mode of maximum growth rate for the range of Rm considered, although it is likely that for higher values of Rm the most unstable mode could shift to $k = 3.0$. Table 1 shows for each run the applied values of the diffusivities ν and η and the calculated values of Re, Rm, k_c and σ_c.

Two further interesting and important results are apparent from table 1. The first is that the flow remains a candidate for fast dynamo action for higher Re. As the magnetic diffusivity is decreased (Rm increased) σ_c (maximized over all k) stays bounded away from zero. Indeed the growth rate at fixed k begins to saturate (increase only slowly) for $Rm \sim 2000$. The strong interacting vortices that are observed for all values of Re are very successful dynamos. Secondly, the dynamo appears to become (slightly) more efficient, i.e. the growth rate increases, for fixed η as ν is decreased. The slight increase is due to the decrease in ν leading to an increase in the flow velocity and hence Rm as η is held fixed. For many dynamo flows this is not the case. In cases where the *flow* is prescribed (i.e. studies of ABC flows Galloway & Frisch 1984), the growth rate is completely independent of the kinematic viscosity ν. In these types of kinematic studies, the velocity is never solved for and the Reynolds number is removed from the problem. In other studies where the forcing is prescribed but adjusted so that in the absence of magnetic field the same flow is forced, the Reynolds number is only important in determining the stability of the basic state to the forcing (see e.g. Brummell *et al.* 2001). The case described here, where the forcing is held fixed as the Reynolds number is increased, allowing ever more turbulent flows to be driven, is analogous to decreasing the kinematic viscosity in convection (while keeping the thermal driving constant).

Perhaps most significantly we find that this dynamo driven by interacting coherent structures remains extremely efficient even when $Re \gg Rm$ (providing $Rm \gg 1$). Table 1 shows that $\sigma_c = 0.543$ for $Re = 2640$, $Rm = 264$. F. Cattaneo (private communication) has shown that for Boussinesq convective dynamos, the dynamo switches off if $Re \gg Rm$. As the Reynolds number increases, the lengthscale of the velocity structures in the convection becomes smaller than those for the magnetic field. This leads to significant cancellation in the magnetic field generation and enhanced diffusion, and hence less efficient dynamo action. The difference for the vortex dynamos, which enables the system to be an effective dynamo even if $Re \gg Rm$, is the presence of an inverse cascade leading to the formation of coherent vortices for all values of Re. These large-scale coherent features can remain efficient generators of magnetic field. This result indicates that the formation of coherent structures in turbulence may be a key feature for magnetic field generation for flows where $Re \gg Rm$ such as those in the solar interior.

5. Conclusions and future work

In this paper we have examined the kinematic dynamo properties of interacting vortices. We considered a $2\frac{1}{2}$-dimensional flow that was driven by steady helical forcing. The velocity evolved from an initially random velocity field via an inverse cascade. The horizontal flows formed vortex patches. The vertical velocity acts as a (signed) passive scalar and becomes aligned with the vertical component of the

vorticity. The fluid Reynolds number was set high enough that the resulting flows are highly time-dependent and turbulent, but the turbulence is dominated by the interaction of the vortices. Calculating the finite-time Lyapunov exponents showed that these flows have the chaotic Lagrangian particle paths required for fast dynamo action. This type of flow is characteristic of astrophysical and geophysical systems, especially in the presence of rotation or stratification. These interacting vortices were shown to be efficient kinematic dynamos by examining the growth of a small-scale random seed field. The mode of maximum growth rate for the field was found to stay at $O(1)$ lengthscales as Rm was increased. This is in contrast to previous models of vortex dynamos consisting of a single vortex tube where the scale of the field along the tube decreases as Rm is increased (Gilbert 1988). Moreover the present flows were shown to be efficient small-scale dynamos for small values of the diffusivities (i.e. large Re and Rm). The optimized growth rate appears to be bounded away from zero as Rm increases and so these flows are very good candidates for fast dynamos. The flows continue to be efficient dynamos even if $Re \gg Rm$ (providing Rm is sufficiently large). The formation of coherent structures in the turbulence is of vital importance, increasing the lengthscale and timescale of the flow and enabling sustained induction and efficient dynamo action. Of course we should stress here that we have considered a sub-class of flows where we allow small scales in two dimensions but not in the third invariant dimension. What we have shown is that the formation of coherent structures in these two dimensions allows dynamo action. The velocity field we have constructed has a spectrum of scales in two dimensions (including some power at large wavenumbers), but still remains an efficient dynamo – we believe due to presence of coherent structures. Investigations of the role of coherent structures in dynamos are currently being performed by analysing the dynamo properties of flows with identical spectra in phase space, but different representations in configuration space.

Again this is of interest geophysically and astrophysically – the presence of rotation or stratification can lead to the formation of coherent structures and these may be the primary players in such dynamos. In fact, rotation and stratification are crucial because they lead to enhanced two-dimensionality of the flow, and hence to quasi-two-dimensional dynamics which support an inverse cascade, although a flow with non-zero vertical velocity is crucial for dynamo action. It is this cascade that leads to the formation of coherent structures.

There are many possible extensions to the calculations above that will be investigated in subsequent papers. It is of course of primary interest to determine the saturation of such dynamos via the nonlinear Lorentz force. Does the dynamo saturate by the subtle mechanism of suppression of Lagrangian chaos (e.g. Cattaneo *et al.* 1996) or simply by modifying the Eulerian motion of the interacting vortices or the formation of coherent structures? This can be investigated within the $2\frac{1}{2}$-dimensional framework by projecting the Lorentz force onto a single mode in the z-direction or in fully three-dimensional simulations. Of course the hydrodynamic stability of the $2\frac{1}{2}$-dimensional flows would also have to be taken into account (e.g. Smyth & Peltier 1994).

Even within the kinematic regime, the role of other geophysical and astrophysical effects are worthy of attention. In the above calculations, the interacting vortices arose as the result of helical forcing. However such interacting vortices may also arise from the instability of shear flows (Hua & Haidvogel 1986). With a constant background shear, there is a continual creation of eddy kinetic energy, that takes the form of vortices. This eddy kinetic energy then cascades up to large scales. The velocity field would then have two components and both the shear and the vortices would be

important in magnetic field generation. The important effects of rotation can also be added by considering quasi-geostrophic flows in the β-plane approximation. Here the energy cascade eventually produces zonal jets. One then expects the flow to have a preferred direction and a net helicity. Flows such as these are not only candidates for small-scale magnetic field generation. A second inverse cascade – mediated by the presence of the net helicity – may lead to the formation of magnetic fields on large scales and shed further light on the problem of field generation in geophysical and astrophysical bodies.

The order of authorship is alphabetical. S. M. T. acknowledges travel support from the Nuffield Foundation. We thank Fausto Cattaneo, David Hughes, Patrice Klein, Michael Proctor and Bill Young for helpful advice.

REFERENCES

Arroyo, P., Pedrizetti, G., Vasco, C. & Jiménez, J. 1995 Statistical properties of decaying two-dimensional turbulence. In *Advances in Turbulence V* (ed. R. Benzi), pp. 11–15. Kluwer.

Babiano, A., Basdevant, C., Legras, B. & Sadourny, R. 1987 Vorticity and passive-scalar dynamics in two-dimensional turbulence. *J. Fluid Mech.* **183**, 379–397.

Balmforth, N. J. & Korycansky, D. G. 2001 Non-linear dynamics of the corotation torque. *Mon. Not. R. Astron. Soc.* **326**, 833–851.

Bassom, A. P. & Gilbert, A. D. 1997 Nonlinear equilibration of a dynamo in a smooth helical flow. *J. Fluid Mech.* **343**, 375–406.

Bracco, A., Chavanis, P. H., Provenzale, A. & Spiegel, E. A. 1999 Particle aggregation in a turbulent Keplerian flow. *Phys. Fluids* **11**, 2280–2287.

Brummell, N. H., Cattaneo, F. & Tobias, S. M. 1998 Linear and nonlinear dynamo action. *Phys. Lett.* A **249**, 437–442.

Brummell, N. H., Cattaneo, F. & Tobias, S. M. 2001 Linear and nonlinear dynamo properties of time-dependent ABC flows. *Fluid Dyn. Res.* **28**, 237–265.

Brummell, N. H., Cattaneo, F. & Toomre, J. 1995 Turbulent dynamics in the solar convection zone. *Science* **269**, 1370–1379.

Brummell, N. H., Clune, T. L. & Toomre, J. 2002 Penetration and overshooting in turbulent compressible convection. *Astrophys. J.* **570**, 825–854.

Cattaneo, F., Hughes, D. W. & Kim, E. 1996 Suppression of chaos in a simplified nonlinear dynamo model. *Phys. Rev. Lett.* **76**, 2057–2060.

Cattaneo, F., Hughes, D. W. & Thelen, J. C. 2002 The nonlinear properties of a large-scale dynamo driven by helical forcing. *J. Fluid Mech.* **456**, 219–237.

Childress, S. & Gilbert, A. D. 1995 *Stretch, Twist, Fold: The Fast Dynamo*. Springer.

Dobler, W., Shukurov, A. & Brandenburg, A. 2002 Nonlinear states of the screw dynamo. *Phys. Rev.* E. **65**, 036311.

Frisch, U. 1995 *Turbulence: the Legacy of A. N. Kolmogorov*. Cambridge University Press.

Galloway, D. J. & Frisch, U. 1984 A numerical investigation of magnetic field generation in a flow with chaotic streamlines. *Geophys. Astrophys. Fluid Dyn.* **29**, 13–18.

Galloway, D. J. & Proctor, M. R. E. 1992 Numerical calculations of fast dynamos in smooth velocity fields with realistic diffusion. *Nature* **356**, 691–693.

Gilbert, A. D. 1988 Fast dynamo action in the Ponomarenko dynamo. *Geophys. Astrophys. Fluid Dyn.* **44**, 241–258.

Godon, P. & Livio, M. 2000 The Formation and Role of Vortices in Protoplanetary Disks. *Astrophys. J.* **537**, 396–404.

Holloway, G. & Kristmannsson, S. S. 1984 Stirring and transport of tracer fields by geostrophic turbulence. *J. Fluid Mech.* **141**, 27–50.

Holloway, G., Riser, S. C. & Ramsden, D. 1986 Tracer anomaly evolution in the flow field of an isolated eddy. *Dyn. Atmos. Oceans* **10**, 165–184.

Hua, B. L. & Haidvogel, D. B. 1986 Numerical simulations of the vertical structure of quasi-geostrophic turbulence. *J. Atmos. Sci.* **43**, 2923–2936.

Hughes, D. W., Cattaneo, F. & Kim, E. 1996 Kinetic helicity, magnetic helicity and fast dynamo action. *Phys. Lett*. A **223**, 16–172.

Kim, E. J., Hughes, D. W. & Soward, A. M. 1999 An investigation into high conductivity dynamo action driven by rotating convection. *Geophys. Astrophys. Fluid Dyn.* **91**, 303–.

Kinney, R. M. & McWilliams, J. C. 1998 Turbulent cascades in anisotropic magnetohydrodynamics. *Phys. Rev*. E **57**, 7111–7121.

Klapper, I. & Young, L. S. 1995 Rigorous bounds on the fast dynamo growth rate involving topological entropy. *Commun. Math. Phys.* **175**, 623–646.

Li, H., Colgate, S. A., Wendroff, B. & Liska, R. 2001 Rossby Wave Instability of Thin Accretion Disks. III. Nonlinear Simulations. *Astrophys. J.* **551**, 874–896.

McWilliams, J. C. 1984 The emergence of coherent isolated vortices in turbulent flow. *J. Fluid Mech.* **146**, 21–43.

McWilliams, J. C. 1990 The vortices of 2-dimensional turbulence. *J. Fluid Mech.* **219**, 361–385.

Moffatt, H. K. 1978 *Magnetic Field Generation in Electrically Conducting Fluids*. Cambridge University Press.

Ohkitani, K. 1991 Wave number space dynamics of enstrophy cascade in a forced two-dimensional turbulence. *Phys. Fluids* A **3**, 1598–1611.

Ponomarenko, Y. 1973 On the theory of hydromagnetic dynamos. *J. Appl. Mech. Tech. Phys.* **14**, 775–778 (English transl.).

Ponty, Y., Gilbert, A. D. & Soward, A. M. 2001 Kinematic dynamo action in large magnetic Reynolds number flows driven by shear and convection. *J. Fluid Mech.* **435**, 261–287.

Provenzale, A. 1999 Transport by barotropic coherent vortices. *Annu. Rev. Fluid Mech.* **31**, 55–93.

Roberts, G. O. 1972 Dynamo action of fluid motions with two-dimensional periodicity. *Phil. Trans. R. Soc. Lond*. A **271**, 411–454.

Roberts, P. H. 1994 Fundamentals of dynamo theory. In *Lectures on Solar and Planetary Dynamos* (ed. M. R. E. Proctor & A. D. Gilbert), pp. 1–58. Cambridge University Press.

Roberts, P. H. & Soward, A. M. 1992 Dynamo theory. *Annu. Rev. Fluid Mech.* **24**, 459–512.

Ruzmaikin, A. A., Sokoloff, D. D. & Shukurov, A. 1988 Hydromagnetic screw dynamo. *J. Fluid Mech.* **197**, 39–56.

Salmon, R. 1998 *Lectures on Geophysical Fluid Dynamics*. Oxford University Press.

Simon, G. W. & Weiss, N. O. 1997 Kinematic modeling of vortices in the solar photosphere. *Astrophys. J.* **489**, 960–967.

Smyth, W. D. & Peltier, W. R. 1994 Three-dimensionalization of barotropic vortices on the f-plane. *J. Fluid Mech.* **265**, 25–64.

Soward, A. M. 1994 Fast Dynamos. In *Lectures on Solar and Planetary Dynamos* (ed. M. R. E. Proctor & A. D. Gilbert), pp. 181–217. Cambridge University Press.

Vincent, A. & Meneguzzi, M. 1991 The spatial structure and statistical properties of homogeneous turbulence. *J. Fluid Mech.* **225**, 1–25.

Vishik, M. M. 1989 Magnetic field generation by the motion of a highly conducting fluid. *Geophys. Astrophys. Fluid Dyn.* **48**, 151–167.

Weiss, N. 2002 Presidential Address: Dynamos in planets, stars and galaxies. *Astron. Geophys.* **43**, 9–3.

Zel'dovich, Y. B. 1956 The magnetic field in the two dimensional motion of a conducting turbulent fluid. *Zh. Exp. Teor. Fiz. SSSR* **31**, 154–155.